International Journal of Heat and Mass Transfer 52 (2009) 3693–3705

Contents lists available at ScienceDirect

International Journal of Heat and Mass Transfer

journal homepage: www.elsevier.com/locate/ijhmt

The physics of heat transfer from hot wires in the proximity of walls of different materials

E.-S. Zanoun [a,*], F. Durst [b], J.-M. Shi [c]

[a] Department of Aerodynamics and Fluid Mechanics, Brandenburg University of Technology Cottbus, Siemens-Halske-Ring 14, D-03046 Cottbus, Germany
[b] FMP Technology GmbH, Am Weichselgarten 34, D-91058 Erlangen, Germany
[c] Siemens AG, Siemens VDO Automotive, SV P GS AD, Siemensstrasse 12, D-93055 Regensburg, Germany

ARTICLE INFO

Article history:
Received 24 April 2006
Received in revised form 14 November 2008
Accepted 2 January 2009
Available online 6 April 2009

Keywords:
Hot wire
Wall proximity
Heat diffusivity

ABSTRACT

This paper concerns the physical process of heat transfer from hot wires located in the proximity of walls consisting of different thermal conductivities. It points out that it is common practice to calibrate hot wires in a free stream of constant and known velocity, but when utilized for near-wall measurements additional heat losses occur owing to the presence of the wall, resulting in erroneous velocity readings. Therefore, a combined experimental and numerical methodology for heat transfer from a heated wire in a flow field is proposed, taking the effects of wire diameter, overheat ratio, wall thermal conductivity, wall distance, wall thickness and shear rate on the measured velocity into account. The present investigations indicated that the flow under the plate, i.e., the corresponding shear rate at the wall opposite the location of the wire where velocity measurements were taken, changes the thermal boundary conditions around the hot wire. It was also observed that heat diffusivity is dominant in the wall region and plays the major role in heat transfer from the wire rather than convection, especially for highly heat-conducting materials. For highly heat-conducting walls, a universal correction law for the wall influence was given by Durst et al. [F. Durst, E.-S. Zanoun, M. Pashtrapanska, In situ calibration of hot wires close to highly heat-conducting walls, Exp. Fluids 31 (2001) 103–110]. However, for poorly heat-conducting walls, the correction law depends on the wall thickness and the heat transfer from the surface opposite the wall where the hot-wire measurements were performed.

1. Introduction and aim of the work

Hot-wire anemometers are widely used in the fluid mechanics community to measure local fluid flow properties. They apply small sensoring wires of a few microns in diameter that are heated to a temperature higher than the fluid to measure the energy loss when exposed to a flowing fluid. In many hot-wire anemometer applications, the pressure and the fluid properties are usually kept constant so that the only variable affecting the convective heat transfer from the wire is the local fluid velocity. For velocity measurements under these conditions, it is common practice to carry out calibrations of the hot wire by exposing it to a free stream of known velocity and of the same fluid as in the actual flow field where velocity measurements need to be carried out. Hence both the calibration fluid and the fluid of the flow to be investigated have the same fluid properties. In this way, a calibration curve $E(U)$ results that can be employed to yield $U(E)$ measurements in unknown flow fields of the same fluid as employed in the calibration. This is the common way to employ hot-wire anemometry in fluid flow investigations.

When hot wires, calibrated in the above manner, are used for local velocity measurements near walls, they experience additional heat losses due to the presence of the wall. This is well known and numerous publications have documented this behavior. In the present paper, the authors' results are presented to give particular attention to the properties of the conductivity of the wall material, the thickness of the wall and the heat transfer that occurs on the wall side opposite the surface where the velocity measurements are carried out. The experimental results show that the conductivity of the wall material has an influence on the hot-wire readings in close proximity to the wall. For poorly heat-conducting wall materials, the resultant hot-wire readings depend also on the thickness of the wall, as mentioned above, and this is confirmed in the present paper.

The authors also performed numerical studies, carrying out computations of the flow field with heat transfer from a wire located close to a flat plate of predefined thickness and material. Fig. 1 shows this arrangement in a manner well suited for setting up the boundary conditions for the computations.

* Corresponding author. Tel.: +49 0355 695127; fax: +49 355 694545.
E-mail address: zanoun@tu-cottbus.de (E.-S. Zanoun).

0017-9310/$ - see front matter © 2009 Elsevier Ltd. All rights reserved.
doi:10.1016/j.ijheatmasstransfer.2009.01.048

Nomenclature

a	overheat ratio ($\Delta T/T_f$)
c_p	specific heat at constant pressure
D	cylinder/wire diameter
E	output of hot wire
g	gravitational acceleration
G	shear parameter
h	heat transfer coefficient
H	wall thickness
H_a, H_b	heights of computational domain
k	thermal conductivity
ℓ	cylinder/wire length
ℓ_c	viscous length scale
L	length of flat plate
P	pressure
$\dot{q}$	specific heat flux
Q_y	diffusion flux
r	cylindrical coordinate/cylinder radius
S	shear rate
t	time
T	temperature
u_τ	wall friction velocity
U	streamwise velocity component
V	normalwise velocity component
x, y	cartesian coordinates
Y	wire-to-wall distance

Greek letters

ρ	fluid density
μ	dynamic viscosity
ν	kinematic viscosity
ϕ	viscous dissipation function
τ	mean wall shear stress
η	normalized wall distance
φ, θ	cylindrical/polar coordinates

Subscripts

c	characteristic quantities
D	wire diameter
f	fluid
m	arithmetic mean/measured/material
x	streamwise distance
w	at the surface of the cylinder/wall
$\infty/0$	at infinity/free stream

Superscripts

$*$	nondimensional quantity
$+$	in wall units

Dimensionless numbers

Bi	Biot number
D	wire diameter
Ec	Eckert number
Gr	Grashof number
Nu	Nusselt number
Pr	Prandtl number
Re	Reynolds number

The figure shows the location of the wire with respect to a solid wall, indicating also the actual flow passing the wire. The lower side of the solid wall is also subjected to a fluid flow. This additional flow was added after the authors' experimental investigations showed that, for poorly heat-conducting wall materials, the wall thickness and the heat transfer at the lower side of the plate showed an influence on the hot-wire readings. This came as a surprise and motivated the research work described here. Although the authors' experiments led to the major findings summarized in this paper, the physical understanding of the phenomena studied was confirmed through the numerical studies, provided in Section 4. To the best of the authors' knowledge, the influence of the wall thickness and heat transfer characteristics at the wall opposite the wire location (i.e., outside the flow field near the wire) has not been studied before. This phenomenon therefore makes the paper useful in treating the hot wire problems in wall proximity both experimentally and numerically.

In Section 2, a summary of the existing knowledge on hot-wire heat transfer is provided. The test rig and the measurements employed are described in Section 3 and the experimental results are summarized. The influence of the wall thickness is explained and information is provided suggesting that numerical investigations are needed to help in understanding the phenomena that occur, and these are provided in Section 4. Section 4.1 gives the equations, numerically, utilized and boundary conditions and also the solution procedure employed. In Sections 4.2 and 4.3, numerical results for conducting and poorly conducting wall materials are given. These results permit an insight into the physical cause and the dependence of the hot-wire readings on the wall thickness and heat transfer characteristics opposite the wall of the wire location.

2. Summary of existing knowledge

The wall proximity effect on hot-wire readings has been classified into either highly heat-conducting or adiabatic walls. Walls which have thermal conductivities much higher than the fluid medium affect, to a great extent, the heat loss from the hot wire by changing the temperature distribution around the wire in the wall region. The wall extracts heat from the fluid which is heated by the wire and this heat loss rapidly increases on approaching the wall. However, in the literature there is a wide scatter and also some discrepancies for wall material effects on hot-wire performance in the vicinity of the wall. For instance, the heat loss from hot wires close to heat-conducting and heat-insulating walls (see Fig. 2a and b, respectively) has been the subject of a large number of experimental, numerical and analytical investigations. Most of these studies agree well with the fact that for $y^+ \leqslant 5$ the hot wire cannot be used without a need for wall corrections. However, a general correction law and application procedure are not deducible from existing data.

Wills in 1962 initiated hot-wire investigations in the proximity of the wall, concluding, at the time of his work, that the heat loss from the wire is related to the Reynolds number and the wall distance normalized by the wire diameter, i.e., y/D. He recommended the corrections for the mean velocity in turbulent flow to be half of the corresponding laminar flow's correction, but without a physical interpretation for this suggestion. In contrast, it was observed by Janke [3] that the mean velocity corrections needed in turbulent flows are still the same as in laminar flows. After Wills [2], Polyakov and Shindin [4] revisited the hot-wire peculiarities near walls of different thermal conductivities (steel, copper and textolite). They showed that the deviation in hot-wire readings is mainly af-

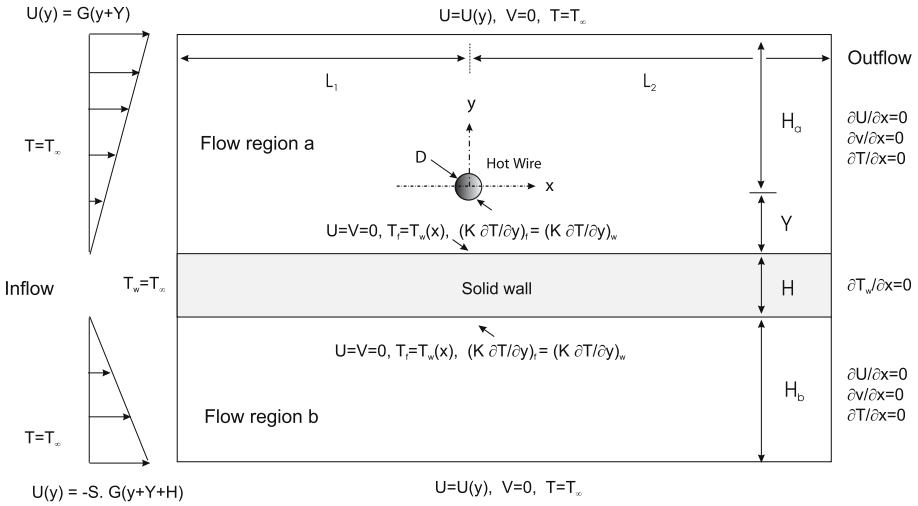

Fig. 1. Sketch of the wire–wall arrangement for numerical investigations.

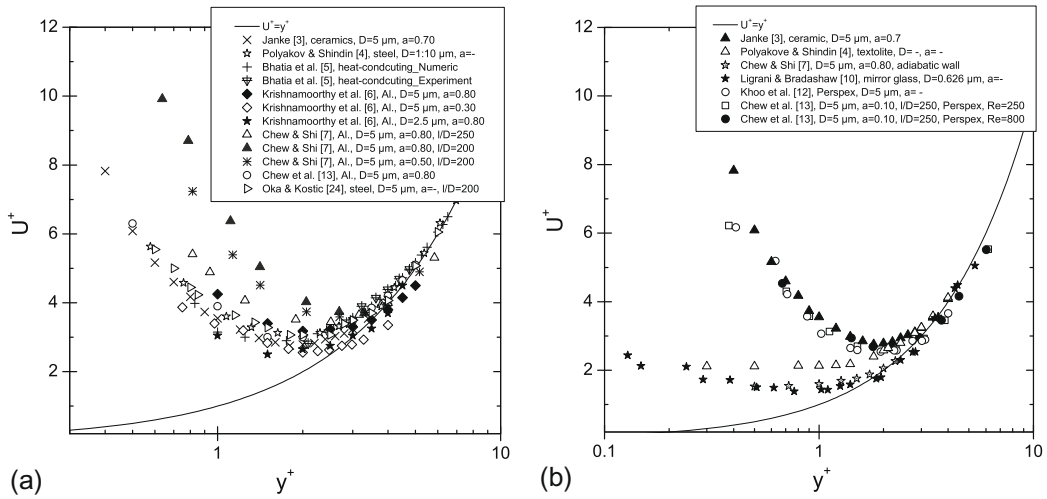

Fig. 2. Comparison of some experimental and numerical findings for the effects of (a) heat-conducting and (b) heat-insulating materials on the normalized velocity distribution near walls.

fected by the thermal and hydrodynamic effects in the vicinity of the wall. The work of Polakov and Shindin [4] was then followed by a numerical study carried out by Bhatia et al. [5] for walls representing ideally conducting and nonconducting (adiabatic) materials. Their corrections were found to be independent of the wall friction velocity, u_τ, when measured data are plotted as $\Delta U^+ = f(y^+)$, and corrections for conducting materials are needed close to the wall, i.e., $y^+ \leqslant 2.5$. However, for nonconducting walls they stated that the heat losses were much smaller and negligible, therefore, no-correction was required according to their numerical study.

Krishnamoorthy et al. [6] conducted a fairly good experimental work taking the effect of wire diameter and overheat ratio on measured velocity near heat-conducting walls. They concluded that corrections needed in the wall proximity are mainly dependent on both the wire diameter and the overheat ratio. However, they failed to evaluate the effect of wire diameter (D) and overheat ratio (a) in terms of Nusselt number (Nu) and Reynolds number (Re). Subsequently, Chew and Shi [7] extended the numerical work of Bhatia et al. [5] with some modifications for the boundary conditions, confirming the wire diameter effect on contrary to an assumption made by Bhatia et al. [5] who neglected the wire diameter effect. Chew and Shi [7], reported in agreement with Chew et al. [8] the effect of overheat ratio as well as wire diameter on heat loss from hot wires in the vicinity of the wall. In addition, they concluded that near-wall corrections are necessary not only for conducting walls but also for adiabatic walls. Earlier work conducted by Zemskaya et al. [9] reported also, in agreement with Chew et al. [8], the effect of overheat ratio on hot-wire measurements in the wall region and concluding that the influence of wire diameter cannot be neglected since it exerts some significant influence on velocity measurements near the wall.

Further investigations by Ligrani and Bradshaw [10] showed that the wire geometry affects turbulence measurements in the wall region. They obtained deviation in velocity measured, starting at $y^+ \leqslant 1.5$ because of the small diameter of their subminiature sensors and the minimal conduction through the mirror glass wall they have used. Moreover, the optimal sensor performance they have obtained was for a wire having an aspect ratio $l/D \approx 260$. In addition, investigations on the effect of walls of different thermal conductivities (metal, wood and Perspex) on hot-wire measurements in the wall region were conducted by Gibbings [11] and Khoo et al. [12]. Khoo et al. [12] introduced experimentally two techniques, namely, laminar flow wall correction and near-wall calibration, claiming that they allowed the realization of true instantaneous velocities near the wall. Their experimental

calibration method had in-situ calibration curve with wall influence calibrated away, i.e., hot wire was calibrated in laminar flow at different distances from the wall substrate (either aluminum or Perspex) for different flow velocities. Therefore, they concluded that the hot-wire performance was fairly independent of both the flow condition and the wall material. Chew et al. [13] continued the work of Khoo et al. [12] and investigated the effect of aluminum and Perspex walls on HWA measurements in a fully developed channel flow. Their effort represented a systematic approach to evaluate wall thermal conductivity, wire diameter and overheat ratio effects on the operation of the hot wire in the vicinity of the wall. In agreement with Durst and Zanoun [14], they observed that the critical distances from the wall beyond which the wall influence is insignificant decreases with decreasing wire diameter and wall thermal conductivity. However, they concluded that the overheat ratio plays an insignificant role and wire of sufficiently large aspect ratio, i.e., $\ell/D \geqslant 200$, minimizes the three-dimensionality effect.

The numerical calculations of Lange [15] and Lange et al. [16,17] were carried out to investigate the correction of hot-wire measurements in the near-wall region of highly heat-conducting and adiabatic walls. They agreed satisfactorily with the experimental data for the effect of wall thermal conductivity, but they concluded that the effect of temperature loading (i.e., overheat ratio) is very small and can be neglected. Durst et al. [1,18] and Durst and Zanoun [14] conducted numerical and experimental studies confirming the wall thermal conductivity effect on hot-wire readings as well as for both the wire diameter and the overheat ratio. More recently, Li et al. [19] conducted a two-dimensional, i.e., for an infinitely long hot wire, numerical study to obtain a correction curve for the near-wall measurements based on thermally insulating (adiabatic) and isothermal walls. They established two dimensionless groupings that influence the near-wall hot-wire operations, expressed in wall units, y^+, and dimensionless parameter accounting for wire height (Y) from the wall normalized by wire diameter (D), i.e., Y/D. Their calculations revealed a possible reason for the apparent discrepancy between the near-wall hot wire correction curves of Chew and Shi [7] and Lange et al. [16,17] next to a thermally nonconducting wall.

In spite of the above efforts, less satisfactory agreement of hot-wire readings was observed close to walls made of insulating materials such as glass, Perspex or Textolite. This was indicated in Fig. 2b, providing extracted information on heat transfer from hot wires close to heat-insulating walls. Controversial conclusions were drawn from a number of the experimental and numerical studies that have been carried out for such heat loss from hot wires close to "heat-insulating walls", e.g., by Wills [2], Polyakov and Shindin [4], Bhatia et al. [5], Ligrani and Bradshaw [10] and Chew and Shi [7]. For instance, Bhatia et al. [5] concluded that no corrections for nonconducting walls are needed since the heat losses are small and negligible, contradicting Chew and Shi [7]. By introducing a special calibration technique, Khoo et al. [12] concluded that the hot-wire performance was fairly independent of both the flow condition and the wall material. Chew et al. [13] continued the work of Chew and Shi [7], deducing larger wall effects as the wall material becomes more thermally conducting. On the other hand, Lange et al. [16,17] and Durst et al. [18] obtained a positive correction for hot-wire readings, i.e., a negative wall effect, close to adiabatic walls. To conclude, Fig. 2 shows that the available data are less consistent, but still provide the following general features:

- Widely scattered and less consistent hot-wire data exist in the vicinity of the wall because of the many influencing factors.
- There is no heat-insulating material that negates the need for hot-wire measurement corrections because of the proximity of the wall.
- The flow pattern, i.e., laminar and/or turbulent flows, near the wall might play a role in the heat transfer from HWA in the wall region.

It seems, therefore, from the above summary, that the wall proximity effect on hot-wire readings has attracted considerable attention, but without revealing a clear and consistent trend for the influence of the wall conductivity. Discrepancies, contradictions and nonuniversality of suggestions for corrections were found. All the above efforts faced difficulties in treating the problem of wall effects on HWA, which might be attributed to the quality of experimental test facilities, their geometric aspects, accuracy of wire calibration in a free stream, wall distance determination, inaccurate wall-shear stress measurements, inappropriate measuring probe or numerical boundary conditions, three-dimensionality effect and flow pattern.

3. Experimental investigations

3.1. Experimental apparatus and hot-wire calibration

A laminar boundary layer was set up in a small Göttinger-type wind tunnel at LSTM-Erlangen using flat plates of different wall materials and configurations. The tunnel was designed for air velocities up to 12 m/s with a background turbulence intensity of the incident flow less than 0.4%. Both sides of the test section consisted of glass walls to provide optical access for the laser beams of the one-dimensional laser Doppler system employed; more details about the entire test facility can be found in Durst et al. [1] and Zanoun [20]. A flat Eloxide aluminum plate was mounted inside the test section, permitting good access to the boundary layer flow for hot-wire investigations near the heat-conducting wall. All the measurements were conducted at 175 mm from the leading edge of the plate for $Re_x \approx 7 \times 10^4$, based on a 6 m/s free stream velocity. Glass and Plexiglas plates of thicknesses 3 and 8 mm were also used to represent walls of heat-insulating materials. All plates were aligned to the flow to yield zero pressure gradient laminar boundary layer flow. Thereafter, laser-Doppler anemometer (LDA), having a control volume (Δy) of 60 μm, which is equivalent to 0.85 in wall units, was used in conjunction with the Blasius velocity distribution in order to make sure that the LDA gives the right distribution of velocity profile and then was applied to calibrate the hot wire. In this sense, it was clear that the hot-wire data lie on the Blasius curve at least away from wall effect and it was also proven through our work, see Durst et al. [1], that the LDA provides good calibration in flow fields with velocity gradients, at least as far as the mean velocities are concerned. Depending on the flow velocity, data rates of 30–300 Hz were typically obtained. For computing the mean velocity of the local flow measurements, 4000–6000 samples were acquired at every measuring station which is large enough for investigating laminar flows.

To carry out the hot-wire measurements simultaneously with the LDA, a DANTEC 55M10 constant temperature anemometer was used. Boundary layer-type hot-wire probes of different wire diameters, 2.5, 5 and 10 μm, having high enough aspect ratios, i.e., $\ell/D \geqslant 200$, were used in all of the measurements. These hot-wire measurements were performed for two different overheat ratios, namely $a = 0.70$ often used for HWA measurements in laminar and turbulent flows, and $a = 0.29$, for comparison with the numerical data. The hot-wire probe was installed about 3 mm downstream of the LDA measuring control volume so as not to disturb the flow at the position where the LDA measurements were conducted. The laser Doppler optical system was operated in the dual-beam forward-scattering mode. In order to ensure that measurements could be made close to the wall, the sending and receiving optics were

tilted about 1° and 2°, respectively, to the plate. To avoid unnecessary light scattering from the wall and to increase the resultant signal-to-noise ratio, the aluminum plate was anodized to yield a black, non-shiny surface. The treated layer was very thin so that the thermal conductivity of the wall material could be assumed to be unchanged. In addition, glass and Plexiglass plates were blackened where LDA measurements were carried out, aiming at minimizing light scattering from the wall. The seeding was adjusted to be as low as possible to avoid contamination of the wire, and at the same time to allow measurements with the LDA in a reasonable time.

Each hot-wire probe was calibrated before carrying out velocity measurements against the LDA in the free stream of the same tunnel, yielding an electrical signal which depended on the overheat ratio of the wire and the calibration velocity. Particular attention was paid to the calibration at low flow velocities since the velocity in the near-wall region is usually less than 1 m/s. A fourth-degree polynomial was chosen to fit the calibration data within an accuracy better than ±1%. The temperature of the air stream inside the wind tunnel was kept constant within ±0.2 °C during the calibration procedure and also during the measurements so as to yield accurate hot-wire velocity results. Once the calibration curve had been established and the least-squares curve fitting equation obtained, the flow field measurements were carried out.

3.2. Hot-wire wall positioning approach

It was of vital importance to specify the exact distance of the hot wire from the wall. To determine the wire position, the calibration procedure proposed in Bhatia et al. [5] and Durst et al. [1] was used. This dictates no-flow measurements of the hot-wire output, E, for different wall distances, y, and results are presented in Fig. 3; E_0 is the wire output far from the wall. The results of the position calibration which are shown in Fig. 3 are for a 0.70 overheat ratio utilizing three wire diameters over two different wall materials. Data points next to the wall surface were fitted linearly. The linear parts of the calibration curves were used later to determine the exact distance of the wire from the plate by moving the plate as close as possible to both the LDA and HWA (less than 100 μm) and the wire output was then measured. From the position calibration lines shown in Fig. 3, the corresponding position of the wire was exactly estimated.

3.3. Experimental results for heat-conducting and heat-insulating materials

It is common to represent the heat transfer from the hot wire in a general form, i.e., in the form of a Nusselt–Reynolds numbers (Nu_m–Re) diagram (see Fig. 4), as suggested by King [21], Nusselt [22], Collis and Williams [23] and Wills [2]. Dimensional analysis was carried out [20], showing that the appropriate length and velocity scales are the viscous length, $l_c = \nu/u_\tau$, and the friction velocity, u_τ, respectively. The wall shear stress, $\tau_w = -\mu \mathrm{d}U/\mathrm{d}y$, was deduced from the gradient of the mean velocity profile in the near-wall region measured by the LDA. Hence, the wall friction velocity, $u_\tau = \sqrt{\tau_w/\rho}$, used for scaling hot-wire data was obtained independently from the hot wire velocity measurements. As a result, the measured vertical distances from the wall and the wire diameter were scaled with the viscous length scale to give $y^+ = yu_\tau/\nu$ and $D^+ = Du_\tau/\nu$, respectively. Also, the measured velocities were scaled with the wall friction velocity to yield $U^+ = U/u_\tau$. A summary of the nondimensional heat transfer data from hot wires is presented in Fig. 4 in the form of Nu_m–Re, where the Reynolds number is defined as $\mathrm{Re}_D = D^+y^+$ (i.e., $\mathrm{Re}_D = DU/\nu = (Du_\tau/\nu)(U/u_\tau) = D^+U^+ = D^+y^+$), since in the viscous sublayer $U^+ = y^+$. As a result, the heat transfer from the hot wire of a high enough aspect ratio shows the following general dependence of the Nusselt number on the other dimensionless quantities:

$$\mathrm{Nu}_m = f\left(y^+, D^+, \frac{\Delta T}{T_f}\right). \tag{1}$$

The experimental investigations were performed to prove that the influence of the normalized parameters expressed in Eq. (1) exists. A sample of the results is presented in Fig. 4 for hot wires close to (a) heat-insulating and (b) heat-conducting walls. The figure shows that the presence of the wall strongly influences the heat loss from hot wires and this effect increases with decreasing wall distance, increasing wire diameter and overheat ratio, $\Delta T/T_f$.

To clarify the influence of the wire diameter on the hot-wire performance, measurements were carried out for the same overheat ratio, but for different wire diameters. In a similar way, the effect of overheat ratio was studied by keeping the wire diameter constant and varying the wire temperature. Two sets of data are presented in Fig. 5a and b for two different overheat ratios, 0.70 and 0.29, and three different wire diameters over highly heat-conducting wall material. Close to the wall surface, a deviation in hot-wire readings was observed; elsewhere there was good agreement with the LDA data and the theoretical line $U^+ = y^+$ up to $y^+ \approx 10$ which corresponds to $\eta = y\sqrt{U_\infty/x\nu} = 1.04$ in the Blasius velocity profile, see Durst et al. [1]. Higher apparent velocities close to the wall were obtained owing to the additional heat losses from the wires due to the thermal conductivity of the wall material. The

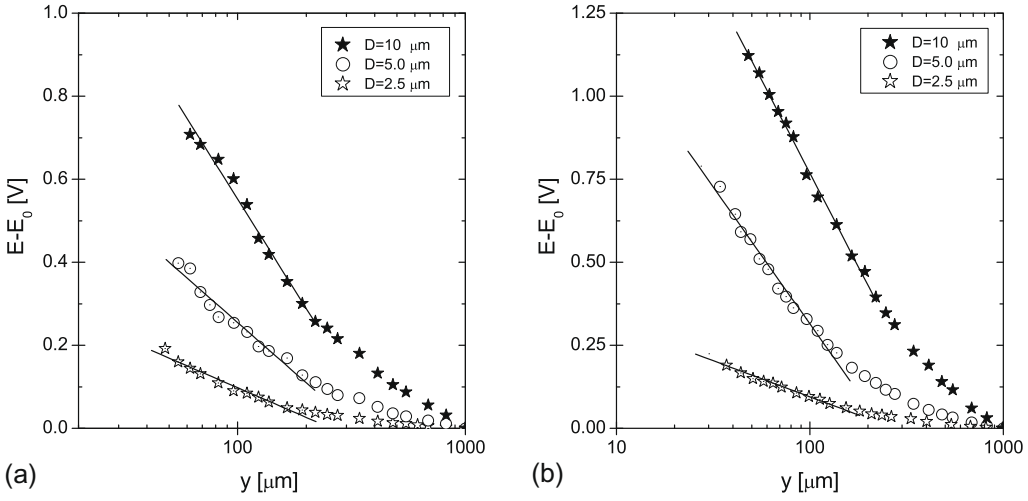

Fig. 3. Position calibration results for hot wires: HWA output versus wire position: (a) heat-insulating (glass) wall and (b) heat-conducting (aluminum) wall.

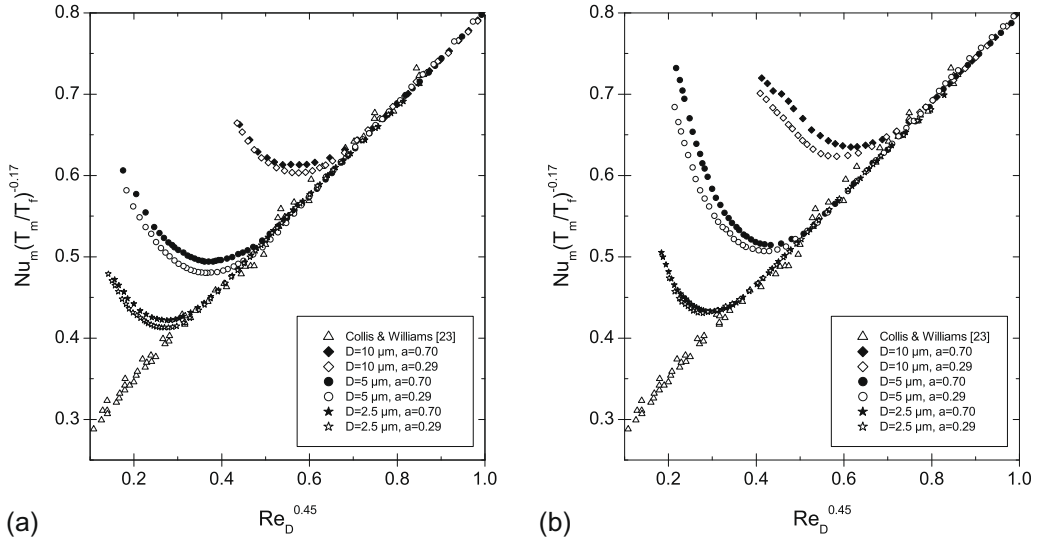

Fig. 4. Heat transfer results from hot wires near (a) a glass wall and (b) an aluminum wall, expressed by the Nusselt number as a function of the Reynolds number, compared with Collis and Williams' experimental data [23].

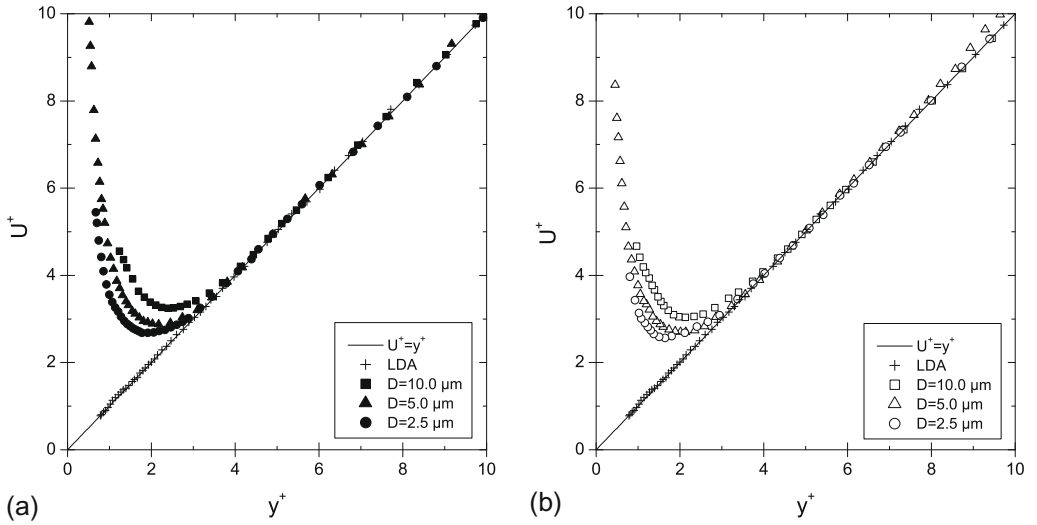

Fig. 5. Effects of wire diameter and overheat ratio, (a) $a = 0.70$, (b) $a = 0.29$, on HWA measured velocity, U^+, along heat-conducting material (aluminum) compared with the linear velocity distribution, $U^+ = y^+$.

heat transfer area of the wire subjected to the wall increases with increasing wire diameter, resulting in higher heat loss to the wall. Moreover, the residence of the air streams heated in the velocity wake directly behind the wire of smaller diameter was shorter compared with the larger wire diameter and consequently more heat was lost to the wall from the large wire diameter. As a result, higher apparent velocities from wires with larger diameters were observed. This reveals a dependence on the wire diameter and therefore the deviation in wire readings increases with increasing wire diameter for a constant overheat ratio. Hence the effect of the wire diameter cannot be neglected since it exerts a significant influence on the velocity and the temperature fields near the wall, see, e.g., Durst et al. [1], Oka and Kostic [24], Hebbar [25], Krishnamoorthy et al. [6], Janke [3] and Chew et al. [13]. This dependence was also observed in [23] and [7]. On the other hand, Bhatia et al. [5] neglected the wire diameter effects, claiming that a wire of very small diameter has no influence on the flow field, i.e., its velocity wake is negligible, and therefore its influence diminishes.

Hence, it was concluded that hot-wire measurements in the wall proximity show wall effects on measurements which depend on both the overheat ratio and the wire diameter. This can be clearly seen from the results presented in both Figs. 4 and 5 and as predicted from Eq. (1). Both figures indicate, as expected, that the additional heat loss from the wire in the presence of the wall increases with increasing overheat ratio. However, this dependence gradually decreases with decreasing wire diameter, see, e.g., Durst et al. [1] and Durst and Zanoun [14]. Such a dependence on the overheat ratio increases as the diameter of the wire increases, for the reasons explained earlier, in addition to the high velocity gradient which exists close to the wall and along the wire diameter as well. The effects of the overheat ratio and the wire diameter on the heat loss from hot wires in the vicinity of the highly heat-conducting walls were also reported by others, Chew and Shi [7], Krishnamoorthy et al. [6], and Zemskaya [9]. However, it was concluded by Chew et al. [13] that no apparent influence was observed when the overheat ratio changed. The present

results, therefore, give the expected trend for both the wire diameter and the overheat ratio effects.

Fig. 6 compares the present data for hot-wire readings close to highly heat-conducting walls with the results extracted from the literature. The chosen sets of the present data shown in Fig. 6 were carried out with a 5-μm diameter wire and compared with others for almost the same overheat ratio, showing satisfactory agreement. The differences among the results can be attributed to differences in the wall thermal conductivities (e.g., $k_{aluminum}$ = 204–237 W/m K and k_{steel} = 15–55 W/m K; see, e.g, Eckert [26]), quality of experimental test facilities and their geometric aspects such as channel aspect ratio and channel height, accuracy of hot-wire calibration in the free stream, differences in wire geometry and wall distance measurements. The same conclusion was obtained for measurements near heat-insulating materials; see, e.g., Durst and Zanoun [14] and Zanoun [20].

To provide further insight into the use of hot wires close to walls, the cause of the additional heat losses from hot wires close

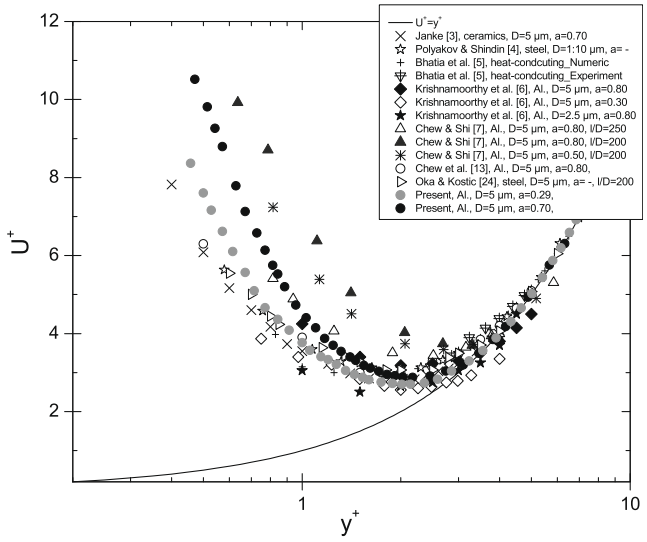

Fig. 6. Comparison of the present results with others showing the effect of the heat-conducting materials on the measured normalized velocity distribution in wall proximity.

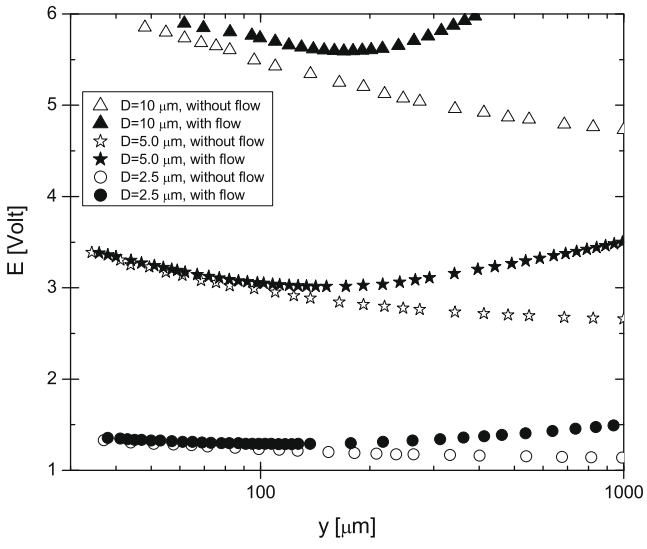

Fig. 7. Hot-wire output with and without flow close to a metal (aluminum) wall for a 0.70 overheat ratio.

to metal and insulating walls was physically explained by carrying out experiments using hot wires with and without flows. Fig. 7 shows the influence of heat conduction and free convection on the hot-wire readings over a horizontal flat plate made of aluminum standing under the wire in absence of the flow. The figure presents results obtained without flow for wires of 2.5, 5 and 10 μm diameter and for a common overheat ratio of 0.70. Under flow conditions, the figure also indicates the heat loss from the wire by forced convection. The figure clearly shows, for zero flow velocity, the dominance of heat conductivity close to metal walls for wall distances $y < 100$ μm. The dominance of heat conductivity in the wall region remains and this is clearly shown by the fact that the two sets of data, i.e., with and without flow, in Fig. 7 are close to each other for the last 100 μm of the 3 mm boundary layer thickness. By looking at the normalized energy equation for steady flow conditions:

$$\underbrace{U_i^*\frac{\partial T^*}{\partial x_i^*}}_{I} = \underbrace{\left(\frac{1}{\mathrm{RePr}}\right)k^*\frac{\partial^2 T^*}{\partial x_i^{*2}}}_{II} + \underbrace{\left(\frac{\mathrm{Ec}}{\mathrm{Re}}\right)\phi^*}_{III}, \tag{2}$$

it was observed that most of the heat went into the metal wall because of the heat diffusion term (II) in Eq. (2) for constant Pr. Small velocities exist in the wall region and therefore the heat loss by free convection may be neglected if $\mathrm{Gr} < \mathrm{Re}_D^3$; see, e.g., [23]. In common agreement with [23] using hot wires in the wall region, the Grashof number in the present investigations was found to be of the order of 10^{-7} and the Reynolds number of the order of 10^{-2}; therefore, the condition under which free convection becomes insignificant is satisfied. Hence, in the wall region diffusivity is dominant and consequently the main role is played by heat diffusion rather than forced and/or free convection.

However, it was observed that the influence of convection on the heat transfer from the 10-μm hot wire is still non-negligible for wall distances $y < 100$ μm. Results for the 10-μm diameter wire with an overheat ratio of 0.70 presented in Fig. 7 indicate a noticeable influence of the flow. This might be explainable by looking at the ratio between the heat loss by diffusivity and convection:

$$\frac{\text{Heat diffusivity}}{\text{Heat convection}} = \frac{\mathrm{Re}_D}{\mathrm{GrPr}} = \frac{1}{D^2}. \tag{3}$$

By introducing the definitions of the Grashof and Reynolds numbers into Eq. (3), it turned out quite clear that the ratio of diffusivity to convection varies as D^{-2}. As a result, increasing the wire diameter resulted in an increase in convection effect in comparison with the corresponding diffusion. Hence, for larger wire diameters and also due to the velocity gradient, there is still a small influence of convective heat transfer from the wire in the vicinity of the wall as a consequence of increasing both the Grashof and Reynolds numbers.

In addition to the above findings, measurements were repeated close to glass walls to demonstrate the importance of heat conductivity in comparison with heat convection and the results are presented in Fig. 8. It turns out that the heat convection in the proximity of heat-insulating materials cannot be neglected when Fig. 8a (a = 0.29) is compared with Fig. 8b (a = 0.70). Applying a higher overheat ratio (i.e., a = 0.70) above the glass plate with and without flow produces a larger difference between glass and aluminum for heat loss by convection. Nevertheless, in the case of heat-insulating materials, the local heat loss from the wire by conduction is much less in comparison with walls of highly heat-conducting materials for the same Re and Pr, since the local heat loss by diffusivity $(k^*/\mathrm{RePr})(\partial^2 T^*/\partial x_i^{*2})$ is strongly dependent on the wall thermal conductivity. The local heat transfer from the wire by conduction is therefore much less in the case of heat-insulating materials compared with walls of highly heat-conducting materi-

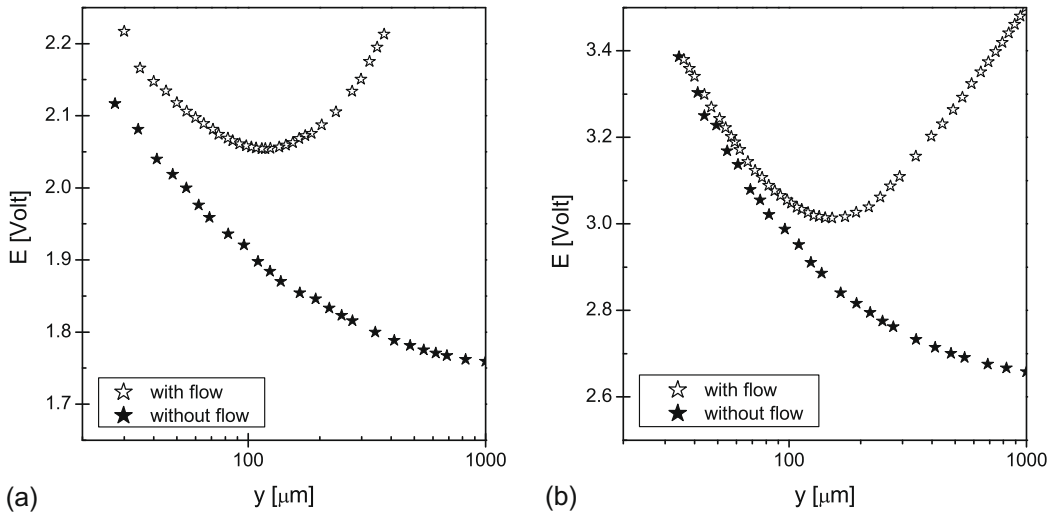

Fig. 8. Conductive and convective effects on hot-wire readings in the proximity of the wall: (a) poorly heat-conducting material (glass), $a = 0.29$ and (b) heat-conducting material (aluminum), $a = 0.70$.

als under the same boundary conditions; see Durst and Zanoun [14] and Zanoun [20]. Therefore, convection heat transfer plays a significant role in the proximity of heat-insulating wall materials in addition to heat conduction.

Apparent inconsistencies in the available data (Fig. 2b), when compared with the present results might be explainable by the effect of the wall thickness which was found in Durst and Zanoun [14]. To explain the role played by the wall thickness on hot-wire readings, it is necessary to consider the heat transfer from the hot wire to the wall material as follows:

$$\rho_m c_{Pm} \frac{\partial T}{\partial t} = k \frac{\partial^2 T}{\partial x_i^2}, \tag{4}$$

where c_{Pm} is the specific heat of the wall material at constant pressure and ρ_m is the density of the wall material. Hence, by considering two flat plates of the same thermal conductivity, but having different wall thicknesses H_1 and H_2, where $H_2 > H_1$, and normalizing Eq. (4) yields the following time-scale ratio of heat conduction through the wall:

$$\frac{(t_c^*)_{H_2}}{(t_c^*)_{H_1}} = \left(\frac{H_2^*}{H_1^*}\right)^2. \tag{5}$$

Therefore, a thinner wall has a smaller conduction time-scale and therefore shows a faster heat loss that is usually carried out by flow under the plate, i.e., at the wall opposite the location of the wire where velocity measurements were taken, than a thicker wall. From the simple laws of heat transfer through wall materials, the overall heat transfer coefficient is inversely proportional to the wall thickness and, consequently, a thinner wall has a smaller thermal heat resistance (i.e., higher conduction rate) than a thicker wall. In addition, a heat-insulating wall accumulates heat inside its material, causing the wall temperature to increase and consequently the thermal conductivity of the wall material decreases because of the increasing the wall temperature. Overall, the conductivity of the thicker wall becomes lower than that of the thinner wall and therefore there is less heat transfer from the hot wire to the thicker wall; see Fig. 9, particularly for $y^+ < 2$. In addition, for heat-insulating materials, the more heat accumulation within the thicker wall modifies more the temperature field around the wire and therefore produces a smaller temperature gradient and as a result less heat transfer from the hot wire to the wall.

4. Numerical computations

The experimental investigations for poorly conducting wall materials showed an influence for both the wall thickness and the heat transfer at the wall opposite the wire location on the hot-wire readings. This motivated, therefore the authors to carry out the numerical simulation to gain some physical insight into this phenomenon. To the best of the authors' knowledge, the influence of the wall thickness and heat transfer characteristics at the wall opposite the wire location, which is outside the flow field has been not numerically studied before. A dimensional analysis in Shi [27] indicated that the wall material, the shear rate and the heat transfer on the wall surface opposite the side where measurements were carried out have potential effects on the heat loss from the hot wire. The effects of these influencing parameters in addition to the wall thickness were observed in the experimental study of Durst and Zanoun [14] for walls of poor thermal conductivity. Therefore, the numerical investigation was performed to confirm the experimental findings in [14]. With the configuration shown in Fig. 1 for the numerical model, the surface thermal condition on the side opposite the wire location was easily varied by changing the flow velocity, i.e., $U(y) = -S \cdot G(y + Y)$, where $S = U_\infty / Y$ is the shear rate and $G = (Y/D)^{-1}$ is the shear parameter, see Shi [27] for more details.

4.1. Mathematical model and solution procedures

The mathematical model describing the flow field around the wire requires considering the governing equations for the mass, momentum and heat transfer expressed in the Cartesian coordinate system as follows:

$$\frac{\partial(\rho^* U_i^*)}{\partial x_i^*} = 0, \tag{6}$$

$$\frac{\partial(\rho^* U_i^* U_j^*)}{\partial x_i^*} = -\frac{\partial P^*}{\partial x_j^*} + \left(\frac{1}{\mathrm{Re}}\right) \frac{\partial}{\partial x_i^*} \left[\mu^* \left(\frac{\partial U_j^*}{\partial x_i^*} + \frac{\partial U_i^*}{\partial x_j^*}\right)\right], \tag{7}$$

$$c_p^* \frac{\partial(\rho^* U_i^* T^*)}{\partial x_i^*} = \left(\frac{1}{\mathrm{RePr}}\right) \frac{\partial}{\partial x_i^*} \left(k^* \frac{\partial T^*}{\partial x_i^*}\right), \tag{8}$$

where $i, j = 1, 2$ are the indices for the coordinate components x and y, respectively. In the above equations, the velocity components and coordinates are normalized by the incoming flow velocity at the

wire height, U_∞, and the wire diameter, D, respectively. The quantities ρ^*, μ^*, k^* and c_p^* are dimensionless physical properties of the air normalized by the corresponding values, namely $\rho_\infty, \mu_\infty, k_\infty$ and $c_{p\infty}$, evaluated at ambient temperature, T_∞, respectively. They were approximated as quadratic polynomial functions of the temperature T [28], based on data from the *VDI-Wärmeatlas* [29], and $T^* = (T - T_\infty)/(T_w - T_\infty)$ is the dimensionless temperature. The dimensionless groups that appear in the above governing equations are the Prandtl number and the Reynolds number, defined as

$$\mathrm{Pr} = \frac{\mu_\infty c_{p\infty}}{k_\infty} = \text{constant} \qquad \text{and} \qquad \mathrm{Re}_{D\infty} = \frac{U_\infty D}{\nu_\infty}, \tag{9}$$

respectively, and the natural convection and viscous dissipation were neglected. Detailed discussions of the physics and justifications for these assumptions and simplifications can be found elsewhere, see, e.g. Bradshaw [30] and Lange [15].

The energy equation is relevant in the proximity of the wall and through the wall material and reduces to the Laplace equation governing the heat conduction by assuming constant physical properties for the solid wall. At the fluid–solid interface, the energy equation is coupled with the temperature and the heat flux conservation, namely

$$T_f^* = T_w^* \qquad \text{and} \qquad \left(k\frac{\partial T^*}{\partial y^*}\right)_f = \left(k\frac{\partial T^*}{\partial y^*}\right)_w. \tag{10}$$

The computational domain was extended in the x-direction to $L_1/D = 8000\text{—}10,000$ upstream and to $L_2/D = 10,000\text{—}12,000$ downstream of the cylinder; see Fig. 1. The height of the computational domain was chosen so that $H_a^+ = H_a u_{\tau,a}/\nu_\infty > 10$ and $H_b^+ = H_b u_{\tau,b}/\nu_\infty > 5$. Such a domain size was found to be sufficiently large to obtain reliable numerical results.

The finite-volume flow solver, FASTEST2D [31], was applied to solve the above equations. A local grid refinement technique was employed to achieve high local resolution near the hot wire and at the same time efficient usage of computational resources. In the present computations, the cylinder ($D = 5$ μm) surface has 512 grid points and about 2.2×10^5 grid points for the total computational domain were applied on the fifth (finest) grid level. Convergence was assumed to be satisfied when the maximum sum of the normalized absolute residuals in all equations was reduced by six orders of magnitude. Analysis of the grid rate of convergence and the grid independence of the numerical results was carried out. Richardson extrapolation [32] was applied to reduce the discretization error. These measures ensured high accuracy of the present results. Detailed information was reported by Shi et al. [33].

The ambient temperature was assumed to be $T_\infty = 20\,^\circ$C. Two wire temperatures, $T_w = 100$ and 166.5 °C, were used for the investigation, corresponding to overheat ratios $a = 0.27$ and 0.50, respectively. The Reynolds number range was $0.001 \leqslant \mathrm{Re}_D \leqslant 2$ and the resulting wall distance in wall units covered the range $0.32 \leqslant y^+ \leqslant 8$. In order to examine the effect of the flow conditions below the plate (region b) on the heat transfer from the hot wire, the shear rate below the wall was varied with a factor of $S = 1$, 0.1 and 0.025 (see Fig. 1). In the case of $a = 0.27$, the numerical results were obtained for two wall thicknesses, namely $H = 3$ and 8 mm, and for three distance-to-diameter ratios, $Y/D = 10, 20$ and 100. Suitable combinations of Re_D and Y/D allowed the dimensionless wire diameter $D^+ = Du_\tau/\nu$ to be varied by changing the shear velocity, u_τ, for a fixed value of Y^+ with reference to the relations $D^+ = \sqrt{\mathrm{Re}_D/(Y/D)}$ and $Y^+ = \sqrt{\mathrm{Re}_D(Y/D)}$, see [27]. Hence both the influence of the model configurations and the shear velocity (u_τ) effect on HWA near-wall measurements were investigated in detail. At each Y^+, numerical results for three different values of D^+ are available, which are sufficient to reveal the influence of D^+ owing to variations of u_τ.

The heat transfer, $\dot{q}(\theta)$, from the hot wire is characterized by the local Nusselt number, $\mathrm{Nu}(\theta)$, which is defined as follows based on the local heat transfer rate at the wire surface:

$$\dot{q}(\theta) = h(\theta)(T_w - T_\infty) = -k(T_w)\left.\frac{\partial T(r,\theta)}{\partial r}\right|_{r=D/2}, \tag{11}$$

where r and θ are the polar coordinates originating at the wire center and $h(\theta)$ is the local heat transfer coefficient at the wire surface. Normalizing $\dot{q}(\theta)$ with a reference value, $\dot{q}_c = k_c(T_w - T_\infty)/D$, one obtains

$$\mathrm{Nu}(\theta) = \frac{\dot{q}(\theta)}{\dot{q}_c} = \frac{h(\theta)D}{k_c} = -\frac{k(T_w)}{k_c}\left.\frac{\partial T^*(r^*,\theta^*)}{\partial r^*}\right|_{(r^*=0.5)}. \tag{12}$$

The mean Nusselt number can be calculated by averaging the local value over the cylinder surface:

$$\mathrm{Nu} = \int_0^1 \mathrm{Nu}(\theta^*)\mathrm{d}\theta^*, \tag{13}$$

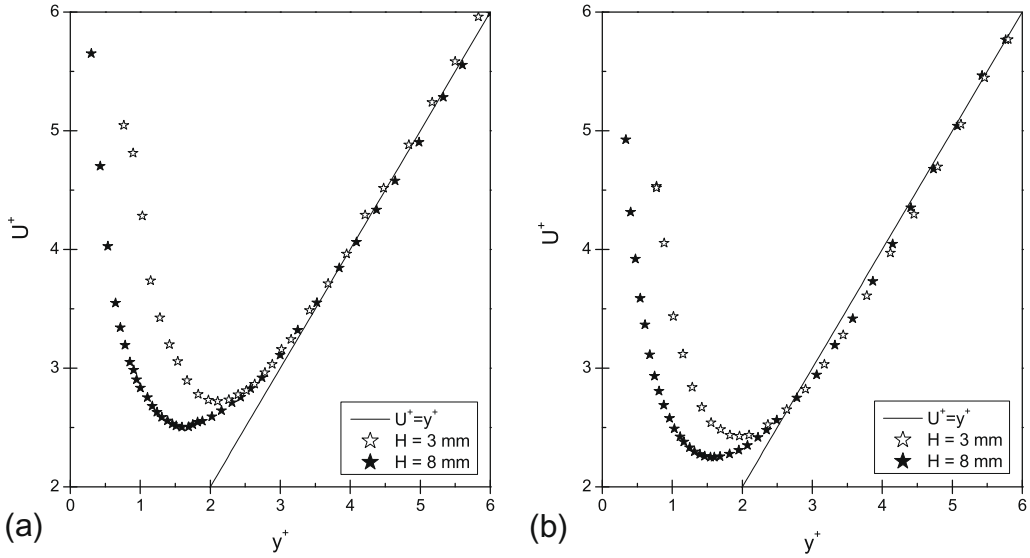

Fig. 9. Wall thickness effect on heat transfer from a hot wire in the proximity of a glass plate for two overheat ratios, (a) $a = 0.70$ and (b) $a = 0.29$.

where $\theta^* = \theta/(2\pi)$. Choosing $k_c = k(T_w)$ for the definition in Eq. (12), the Nusselt number $\mathrm{Nu}(\theta)$ shows a dependence on the dimensionless temperature gradient only at the wire surface.

A numerical calibration procedure was introduced and hence for each given overheat ratio, a reference curve was established for the Nusselt number of the wire in a free stream depending on the wire Reynolds number. By comparing the Nusselt number of the wire in the near-wall region with the corresponding reference curve, the apparent velocity reading of the wire can be determined; see Shi et al. [33] for more details.

For a better understanding of the wall effect on the heat transfer from the hot wire, the distribution of the dimensionless temperature, $T_w^* = (T_w - T_\infty)/(T_w - T_\infty)$, and the dimensionless heat flux at the fluid–wall interfaces, $[y^* = -Y/D, \text{and} -(Y+H)/D]$, was analyzed, i.e.,

$$Q_y = \frac{(k\frac{\partial T}{\partial y})_w}{k_\infty \frac{T_w - T_\infty}{\ell_c}} = \frac{k_w^*}{\mathrm{Re}_D \mathrm{Pr}} \left(\frac{\partial T^*}{\partial y^*}\right)_w, \tag{14}$$

where ℓ_c is defined as $\ell_c = D/(\mathrm{Re}_D \mathrm{Pr})$ and, consequently, Q_y is equivalent to the diffusion integral of the energy Eq. (8) and thus reflects directly the wall influence on the heat transfer from the wire. In addition, a quantity called the modified Biot number, Bi, was introduced and defined as follows:

$$\mathrm{Bi} = \frac{h_w \ell_c}{k_w} = \frac{1}{\mathrm{Re}_D \mathrm{Pr}} \frac{(\partial T^*/\partial y^*)_w}{T_w^*}, \tag{15}$$

expressing the heat flux at the fluid–wall interface, where

$$\dot{q}_w = \left(k_w \frac{\partial T}{\partial y}\right)_w = h_w (T_w - T_\infty), \tag{16}$$

Physically, Bi characterizes the ratio of the convective thermal resistance in the fluid to the conductive thermal resistance inside the solid material and hence it is useful for understanding the effect of the experimental conditions on the HWA near-wall measurements.

4.2. Numerical results for highly conducting wall materials

The numerical results indicate that the effect of the wall thickness on HWA near-wall measurements is negligible in the case of utilizing an aluminum wall. This in fact is true owing to the high thermal conductivity of the aluminum and therefore, the heat exchange at the bottom of the wall is not of interest. The temperature gradient in the solid wall can be neglected for smaller values of the Biot number [34]. Hence, the wall can be assumed to have constant temperature and the thickness of the wall is irrelevant [27]. In agreement with experimental observation, no discernible effect of the wall thickness for the aluminum wall and the incoming flow velocity below the wall on the Nusselt number and thus on the hot wire velocity readings, U^+, was obtained. Moreover, the numerical results were in satisfactory agreement with earlier data of Shi et al. [28] and Durst et al. [18], which were obtained based on a model using $H = 1.5$ mm and the adiabatic boundary condition at the bottom of the wall. The physical cause is implied in the small Biot number values as displayed in Fig. 10. Fig. 10 indicates that the thermal conductivity resistance of the solid wall is small compared with the heat convection resistance in the flow region. In this situation, if $\mathrm{Bi} < 0.1$ according to [34], the wall can be assumed to be of constant temperature and the thickness effect of the wall H is irrelevant, i.e., the wall is *thermally thin*. However, the numerical results obtained using different Y/D, i.e., 10, 20 and 100, corresponding to $D^+ = 0.1, 0.05$, and $0.001Y^+$, respectively, show strong effect of D^+. As demonstrated in Fig. 11 the apparent velocity U^+ increases with increasing D^+, i.e., increasing u_τ or decreasing Y/D, when the wire is located within a wall distance $y^+ \leqslant 4$ from

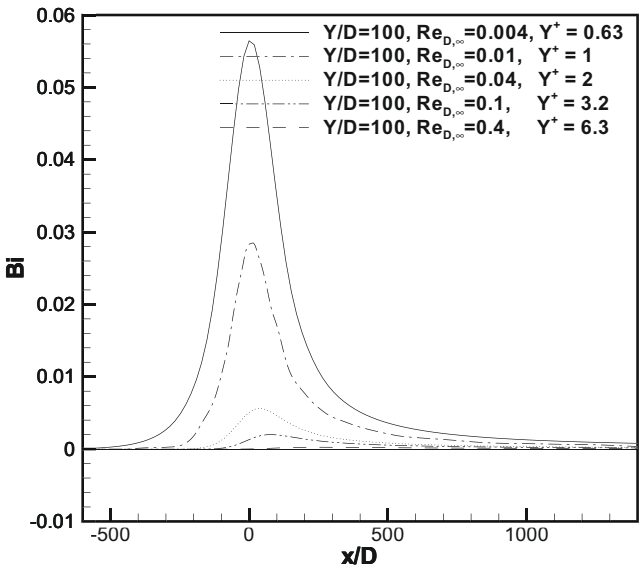

Fig. 10. The modified Biot number (Bi) [Eq. (15)] at the top fluid–wall interface ($y = -Y$) of an aluminum wall ($k_w^* = 9186$).

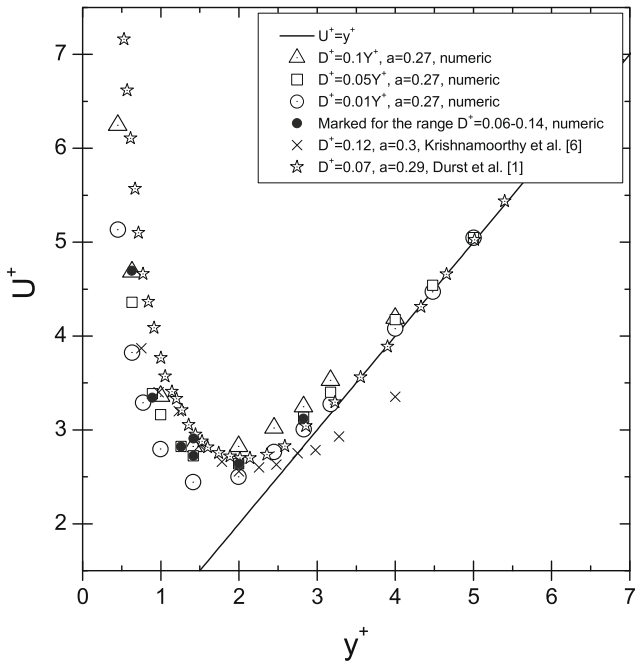

Fig. 11. Comparison of the hot-wire velocity readings for different $D^+(D^+ = Du_\tau/\nu_\infty)$ varied by changing u_τ and Y/D, ($D = 5$ μm and $a = 0.27$).

the aluminum wall. Hence the present results are in agreement with other experimental data of Wills [2], and Gibbings [11], which also indicated an influence for the wall friction velocity, u_τ. Moreover, the numerical results in the parameter range $0.06 \leqslant D^+ \leqslant 0.14$ agree well with the experimental data of Durst and Zanoun [14] ($D^+ = 0.07$) and Krishnamoorthy et al. [6] ($D^+ = 0.12$). The measurements of both Durst and Zanoun [14] ($D^+ = 0.07$) and Krishnamoorthy et al. [6] were carried out using a wire diameter $D = 5$ μm and for a similar overheat ratio to the present numerical study.

4.3. Numerical results for poorly conducting walls

In contrast to highly heat-conducting walls, the numerical results indicate a small effect for the wall thickness, H, and flow

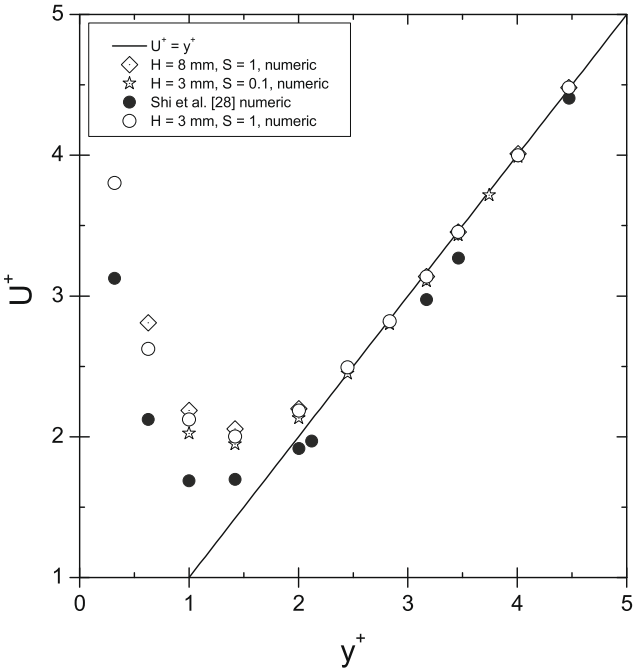

Fig. 12. Comparison of the numerical results of the hot-wire readings close to mirror glass walls ($k_w^* = 29.6$) obtained based on different model configurations, however, for the same $D^+ = 0.01Y^+$ and $a = 0.27$.

condition below the wall in the case of a mirror glass wall ($k_w^* = 29.6$), supporting the experimental observations for the wall thickness effect of poorly conducting materials. Fig. 12 indicates higher apparent velocities in the case of increasing shear rate (S) underneath the plate and this influence is more evident at small wire-to-wall distances, i.e., $y^+ \leqslant 2$. Compared with the present results, the previous study of Shi et al. [28] significantly under-predicted the velocity readings of the wire owing to the inappropriate adiabatic boundary conditions applied at the bottom of the wall and also to the small wall thickness ($H = 1.5$ mm).

The influence of the wall thickness H and the incoming flow velocity below the wall on HWA measurements has been realized by the conjugate thermal boundary condition at the top fluid–wall interface ($y = -Y$). In order to have a clear physical insight into this problem, the distributions of the temperature T^* and the modified Biot number Bi [Eq. (15)] at both fluid–wall interfaces [$y = -Y$ and $y = -(Y + H)$] were analyzed. As an example, the results for the case of $Y/D = 100$ and $\mathrm{Re} = 0.01$ under different flow conditions below the 3 mm glass wall ($S = 0.1, 1$) are displayed in Fig. 13. According to Eq. (15), a positive value of Bi means that there is heat flux entering the solid wall at the top interface or going into the flow region below the wall through the bottom interface. On the other hand, a negative value at the top interface corresponds to a heat feedback from the solid wall to the flow region above the plate. It is also observed that compared with the case of $S = 1$, a reduced flow convection below the wall (i.e., $S = 0.1$) results in higher temperatures at the fluid–wall interfaces; see Fig. 13a. This effect is more evident as indicated in Fig. 13b, where smaller values of Bi were observed for $S = 0.1$, which clearly reflects an increase in the convective thermal resistance $1/h_w$ [see Eq. (15)] in both flow regions.

The effect of the wall thickness H on HWA near-wall measurements can be easily understood based on the results in Fig. 14. Considering that the thermal conductivity of the mirror glass is much larger than that of the fluid ($k_w^* = 29.6$), the heat conduction inside the solid wall in the x-direction (lateral) is expected to become stronger with increasing wall thickness. As a result, the interface temperature near the wire location is found to be lower and with a slower decay in the x-direction (owing to the larger heat supply) in the case of a thicker wall, Fig. 14a. For the same reason, Bi increases with increasing the wall thickness, whereas the heat flux feed back from the solid wall to the flow region a through the top interface ($y = -Y$) or the heat flux transported to the flow region below the wall (b) through the bottom interface ($y = -Y - H$) decreases with increasing H (Fig. 14b).

The numerical results with the corresponding parameter range ($0.06 \leqslant D^+ \leqslant 0.14, a = 0.27$ and $H = 3$ mm) also agree satisfactorily with the experimental data of Durst and Zanoun [14] ($D^+ = 0.07, a = 1.29$ and $H = 8$ mm) in spite of the fact that the thermal conductivity of their wall material (k_w^*) was not known exactly. In Fig. 15, the results from Ligrani and Bradshaw [10] are presented, showing smaller deviations than the others. This smaller deviation may be due to the small dimensions of their hot-wire sensor D^+ ($= 0.013$) and because of the no-flow convection below the wall ($S = 0$). It is worth mentioning also that the thermal conductivity, the wall thickness and the overheat ratio were not given [10].

5. Conclusions

Experimental and numerical simulations of the forced and free heat convection from a heated wire in cross-flow in both a free

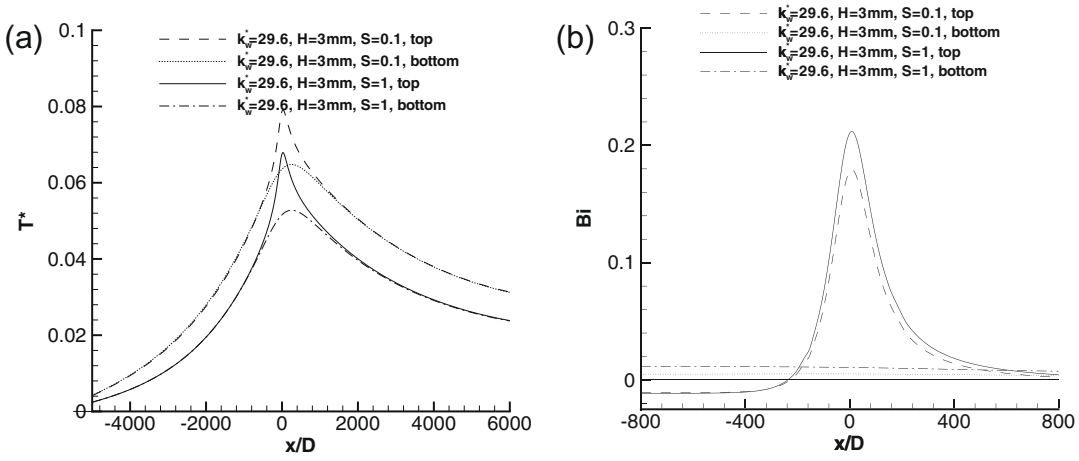

Fig. 13. Effect of the shear rate of the flow region below the wall ($S = 1$ and 0.1) on (a) the temperature T^* and (b) the modified Biot number Bi at the fluid–wall interfaces [top, $y = -Y$, and bottom, $y = -(Y + H)$] in the case of a mirror glass wall ($k_w^* = 29.6$) with a thickness $H = 3$ mm; $D = 5$ μm, and $Y^+ = 1$ resulting from $Y/D = 100$ and $\mathrm{Re}_{D,\infty} = 0.01$.

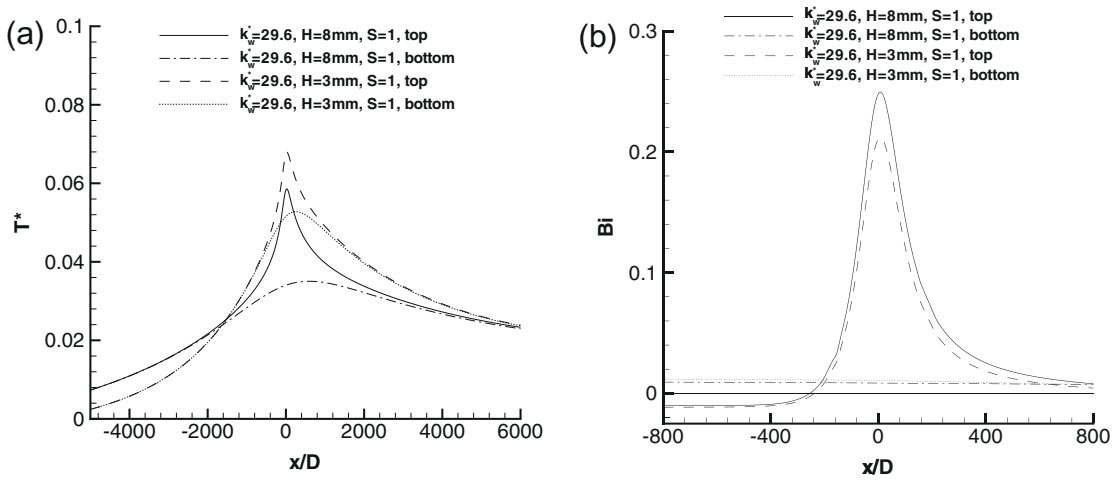

Fig. 14. Effect of wall thickness ($H = 3$ and 8 mm) on (a) the temperature T^* and (b) the modified Biot number Bi at the fluid–wall interfaces [top, $y = -Y$, and bottom, $y = -(Y + H)$] in the case of a mirror glass wall ($k_w^* = 29.6$), $D = 5$ μm, $Y^+ = 1$ resulting from $Y/D = 100$ and $\mathrm{Re}_{D,\infty} = 0.01$.

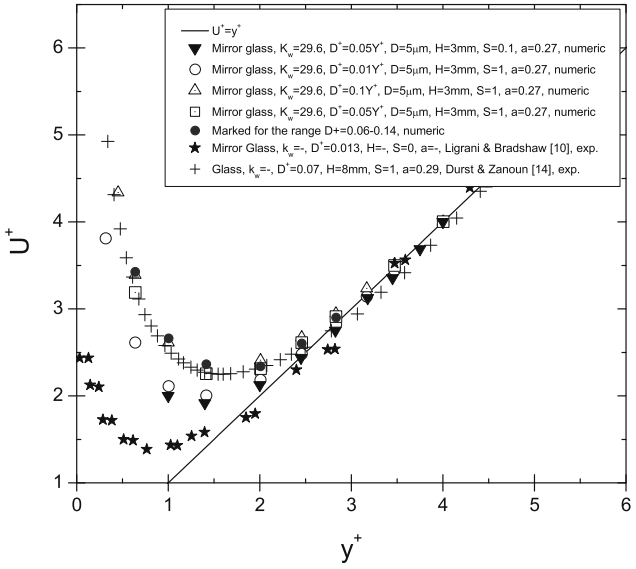

Fig. 15. Velocity readings of the hot wire in the wall proximity, comparison for different $D^+(D^+ = Du_\tau/\nu_\infty)$ varied by the shear velocity u_τ or Y/D, where $D^+ = y^+/(Y/D), D = 5$ μm and $a = 0.27$.

stream and wall proximity of laminar boundary layer flows were carried out to investigate the wall effect on HWA measurements. Particular attention was paid to the influence of the wall thickness (H), the flow conditions at the wall opposite the wire position (varied by the shear rate S), the shear velocity (u_τ), the wire diameter (D) and the overheat ratio (a). An improved physical model was introduced for the phenomena that take the flow region below the solid wall into account in the computational domain, leading to the following conclusions:

1. There is practically no wall material available which permits hot-wire measurements that are free from wall effects. The major effect on heat loss from hot wires close to the wall is due to the wall itself, causing modifications of the temperature field around the wire responsible for the heat conduction. Hence the wall material was found to have the dominant effect on the hot-wire readings in the proximity of the wall. Velocity corrections are then needed if measurements are taken close to heat-conducting materials. But, for heat-insulating materials, corrections turn out to be smaller than that for heat-conducting walls.
2. The wall thickness influence cannot be neglected when a poorly conducting wall is utilized. In another words, for heat-insulating materials, the wall thickness has a significant effect on hot-wire heat losses in wall proximity.
3. The results indicate that the shear velocity u_τ or the equivalent distance-to-diameter ratio Y/D has a significant effect on HWA near-wall measurements. This finding is a new proof to object to a universality of a velocity correction procedure which suggests a single dependence on Y^+, proposed in the literature.
4. The influence of the overheat ratio and the wire diameter cannot be ignored since they significantly affect the hot-wire readings in the proximity of the wall.
5. The present experimental results (Fig. 9) and numerical results confirm the earlier observations of Shi et al. [28] that concern the negative velocity corrections needed for the HWA measurements close to poorly conducting walls.

Extension of the present work, no doubt, is needed to investigate how thick the poorly heat-conducting wall has to be before the effect of the flow field on the opposite wall starts to stop influencing hot-wire readings. In another words, the critical thickness of the poorly heat-conducting wall needs to be well determined. Similarly, the critical value of the shear rate on the opposite side of the wall that influences heat loss from the wire needs to be specified. In addition, the authors would recommend testing the experimental techniques proposed by Khoo et al. [12] in order to compare the outcome with the present results.

Acknowledgements

This work was supported by a fellowship from the German Academic Exchange Service (DAAD) to J.-M. Shi, which is gratefully acknowledged. Thanks also are due to Prof. G. Biswas of the Indian Institute of Technology, Kanpur, for valuable discussions.

References

[1] F. Durst, E.-S. Zanoun, M. Pashtrapanska, In situ calibration of hot wires close to highly heat-conducting walls, Exp. Fluids 31 (2001) 103–110.
[2] J.A.B. Wills, The correction of hot-wire readings for proximity to a solid boundary, J. Fluid Mech. 12 (1962) 388–396.
[3] G. Janke, Hot wire in wall proximity, in: G. Comte-Bellot, J. Mathien (Eds.), Advance in Turbulence, Springer, Berlin, 1987, pp. 488–498.

[4] A.F. Polyakov, S.A. Shindin, Peculiarities of hot-wire measurements of mean velocity and temperature in the wall vicinity, Heat Mass Transfer 5 (1978) 53–58.
[5] J.C. Bhatia, F. Durst, J. Jovanovic, Corrections of hot-wire measurements near walls, J. Fluid Mech. 122 (1982) 411–431.
[6] L.V. Krishnamoorthy, D.H. Wood, R.A. Antonia, R.A. Antonia, A.J. Chambers, Effect of wire diameter and overheat ratio near a conducting wall, Exp. Fluids 3 (1985) 121–127.
[7] Y.T. Chew, S.X. Shi, Wall proximity influence on hot-wire measurements, in: R.M.C. So, C.G. Speziale, B.E. Launder (Eds.), Near Wall Turbulent Flows, Elsevier Science, Amsterdam, 1993, pp. 609–618.
[8] Y.T. Chew, S.X. Shi, B.C. Khoo, On the numerical near-wall corrections of single hot-wire measurements, Int. J. Heat Fluid Flow 16 (1995) 471–476.
[9] A. Zemskaya, V.N. Levitskiy, Y.U. Repik, Y.P. Sosedko, Effect of the proximity of the wall on hot-wire readings in laminar and turbulent boundary layers, Fluid Mech. Sov. Rev. (8) (1979) 133–141.
[10] P.M. Ligrani, P. Bradshaw, Subminiature hot-wire sensors: development and use, J. Phys. E Sci. Instrum. 20 (1987) 323–332.
[11] J.C. Gibbings, The wall correction of the hot-wire anemometer, Flow Meas. Instrum. 6 (1995) 127–136.
[12] B.C. Khoo, Y.T. Chew, G.L. Li, Time-resolved near wall hot-wire measurements: use of laminar flow wall correction curve and near-wall calibration technique, Meas. Sci. Technol. 7 (1996) 564–575.
[13] Y.T. Chew, B.C. Khoo, G.L. Li, An investigation of wall effects on hot-wire measurements using a bent sublayer probe, Meas. Sci. Technol. 9 (1998) 67–85.
[14] F. Durst, E.-S. Zanoun, Experimental investigation of near-wall effects on hot-wire measurements, Exp. Fluids 33 (2002) 210–218.
[15] C.F. Lange, Numerical predictions of heat and momentum transfer from a cylinder in crossflow with implications to hot-wire anemometry, Ph.D. thesis, Institute of Fluid Mechanics, Friedrich-Alexander University of Erlangen-Nuremberg, 1997.
[16] C.F. Lange, F. Durst, M. Breuer, Correction of hot-wire measurements in the near-wall region, Exp. Fluids 26 (1998) 475–477.
[17] C.F. Lange, F. Durst, M. Breuer, Wall effects on heat losses from hot wires, Int. J. Heat Fluid Flow 20 (1999) 34–47.
[18] F. Durst, J.-M. Shi, M. Breuer, Numerical prediction of hot-wire corrections near walls, ASME J. Fluids Eng. 124 (2002) 241–250.
[19] W.Z. Li, B.C. Khoo, D. Xu, The thermal characteristics of a hot wire in a near-wall flow, Int. J. Heat Mass Transfer 49 (2006) 905–918.
[20] E.-S. Zanoun, Answers to some open questions in wall-bounded laminar and turbulent shear flows, Ph.D. thesis, Institute of Fluid Mechanics, Friedrich-Alexander University of Erlangen-Nuremberg, 2003.
[21] L.V. King, On the convection of heat from small cylinders in a stream of fluid: determination of the convection constants of small platinum wires with application to hot-wire anemometry, Philos. Trans. R. Soc. Lond. 214A (1914) 373–432.
[22] W. Nusselt, Das Grundgesetz des Wärmeüberganges, Gesund. Ing 38 (42) (1915) 477–482.
[23] D.C. Collis, M.J. Williams, Two-dimensional convection from heated wires at low Reynolds numbers, J. Fluid Mech. 6 (1959) 357–384.
[24] S. Oka, Z. Kostic, Influence of wall proximity on hot-wire velocity measurements, Dansk Industri Syndikat Aktieselskab Information No. 13, 1971, pp. 29–33.
[25] K.S. Hebbar, Wall proximity corrections for hot-wire readings in turbulent flows, Dansk Industri Syndikat Aktieselskab Information No. 25, 1978, pp. 15–16.
[26] E.R.G. Eckert, M. Robert, J.R. Drake, Analysis of Heat and Mass Transfer, Hemisphere, New York, 1987.
[27] J.-M. Shi, Numerical study of classical low Reynolds number flow problems, Ph.D. thesis, Institute of Fluid Mechanics, Friedrich-Alexander University of Erlangen-Nuremberg, 2002.
[28] J.-M. Shi, M. Breuer, F. Durst, Wall effect on heat transfer from a micro cylinder in near-wall shear flow, Int. J. Heat Mass Transfer 45 (2002) 1309–1320.
[29] Verein Deutscher Ingenieure, VDI-Wärmeatlas, seventh ed., VDI, Düsseldorf, 1994.
[30] P. Bradshaw, An Introduction to Turbulence and its Measurement, Pergamon Press, Oxford, 1971.
[31] F. Durst, J. Shi, M. Schäfer, A parallel block-structured multigrid method for the prediction of incompressible flows, Int. J. Numer. Methods Fluids 22 (1996) 549–565.
[32] J.H. Ferziger, M. Peri ć, Computational Methods for Fluid Dynamics, Springer, Berlin, 1999.
[33] J.-M. Shi, D. Gerlach, M. Breuer, F. Durst, C.F. Lange, Analysis of heat transfer from a single wire close to walls, J. Phys. Fluids 15 (2003) 908–921.
[34] N. Elsner, A. Dittmann, Grundlagen der Technischen Thermodynamik, eighth ed., Akademie Verlag, Berlin, 1993.